About Robustness of an Internal Model-based Disturbance Compensator without SPR-like Conditions*

Qilong Zhang[1] and Yang Wang[1]

Abstract— **Rejection of periodic disturbances is a crucial problem in control systems with many applications. While Internal Model (IM)-based approaches have shown promise, their practical adoption has been limited by a lack of robustness. This paper introduces an IM-based Adaptive Feedforward Controller (AFC) that offers rigorously proven robustness against uncertainties in the disturbance model and environmental noise. In comparison to existing literature, the key novelty lies in establishing robustness guarantees for disturbance model uncertainties and noisy environments, without relying on additional frequency estimators or restrictive assumptions. Specifically, an Input-to-State Stability (ISS) property is established concerning the disturbance frequency parameter error, unstructured input and measurement noise. This enables the application of IM-based methods in practical engineering problems with large modeling inaccuracies and noise. The efficacy of the algorithm is validated through numerical simulations and experimental implementations on an Active Noise Control (ANC) testbed.**

I. Introduction

The problem of rejecting disturbances in periodic signals carries significant importance within the control community, with its significance widely acknowledged across various application domains [1], [2]. In the seminal works of Francis, Wonham, and Davison [3], [4], this issue was classified as a part of output regulation, and the renowned internal model principle (IMP) was formally established. The IMP states that effective disturbance rejection can only be achieved when the controller incorporates a suitably replicated model of the disturbance. Consequently, a multitude of IM-based methods have emerged [5], [6]. While these methods exhibit commendable asymptotic convergence properties in theory, their practical application remains limited compared to approaches based on high-gain observers [7], [8], primarily due to concerns regarding their robustness.

In the realm of disturbance rejection based on IM, robustness holds tremendous importance in addressing uncertainties of the plant model and the disturbance model. Milestone works [9], [10] assumed knowledge of the disturbance model along with information on the frequency response of the plant. Subsequent studies made efforts to adaptively estimate the frequency response online, as reported in [11], [12]. However, these papers overlooked certain considerations regarding the interaction with plant dynamics, treating the plant response as a steady-state mapping. The articles [13], [14] addressed this issue with the sign of either the real or imaginary part of the frequency response at the disturbance frequency. Nevertheless, this requirement still demands the persistence of the sign of the real or imaginary part of the frequency response across the relevant frequency range, commonly known as the strictly positive real-like (*SPR-like*) conditions. Naturally, in the absence of prior knowledge of the disturbance frequency, the assumption of minimum phase [15], [16] is also subject to the *SPR-like* conditions. Until recently, a major breakthrough was achieved through novel mechanisms based on multiple-model adaptive control and switching-based strategies, as outlined in our preliminary work [17], where the necessity concerning the frequency response is notably reduced to an observability condition.

However, when confronted with uncertainties in the disturbance model, most existing solutions either rely on online adaptation techniques [14], [18] or external frequency estimators [19], [20]. Thus, the challenge boils down to how to obtain accurate disturbance model information. Nevertheless, in practical engineering applications, acquiring completely precise external disturbance model information becomes impractical due to limitations imposed by sensor levels and ubiquitous noise. While many frequency estimators guarantee bounded estimation errors under conditions of measurement noise [21], there are few algorithms specifically discussed in the context of robustness against disturbance model errors as well as input/measurement noise. However, this type of robustness enjoys substantial importance in practical engineering applications.

In light of the aforementioned discussions, this paper addresses the challenge of achieving robust disturbance rejection for a highly uncertain linear time-invariant (LTI) single-input single-output (SISO) system, in the presence of unstructured input and measurement noise, as well as imprecise prior knowledge of the external disturbance frequency. Following our previous works [17], [22], this study places particular emphasis on establishing the robustness property to enable practical implementations. Through a rigorous Lyapunov analysis, it has been mathematically proven that the system exhibits the desirable ISS property with respect to three perturbations: frequency parameter error, input noise, and measurement noise. The robustness of the presented algorithm is verified through a series of stringent numerical simulations and hardware experiments conducted on an ANC platform. It is noteworthy that this platform represents a realistic and completely unknown environment. This work provides significant insight into the robustness of IM-based solutions, while also offering immense potential for practical applications in real-world scenarios.

*This work was supported in part by the Yangfan Program of Shanghai, China, under Grant 21YF1429600. *(Corresponding author: Yang Wang.)*

[1]Q. Zhang and Y. Wang are with the School of Information Science and Technology, ShanghaiTech University, Shanghai 201210, China {zhangql1, wangyang4}@shanghaitech.edu.cn

Manuscript 232 submitted to 2024 American Control Conference (ACC).
Received September 26, 2023.

The rest of this paper is organized as follows: Section II formulates the problem and proposes an IM-based adaptive regulator. Section III provides stability and robustness analysis of the closed-loop system. Section IV presents detailed simulation and experimental results.

Notation: $\mathbb{R}_{>0} := \{x \in \mathbb{R} : x > 0\}$. $|\cdot|$ denotes the absolute value of scalars. $\|\cdot\|$ represents the Euclidean norm of vectors and matrices, while $\|\cdot\|_\infty$ is the $\mathcal{L}_\infty$ norm of signals. I denotes the identity matrix with the appropriate dimension. ◁

II. Problem Formulation

Consider an uncertain SISO LTI system, whose dynamics can be described by:

$$\begin{aligned} \dot{x}(t) &= A(\mu)x(t) + B(\mu)\big[u(t) - d(t) + w_I(t)\big] \\ y(t) &= C(\mu)x(t) \\ y_m(t) &= C(\mu)x(t) + w_M(t) \end{aligned} \tag{1}$$

where $x(t) \in \mathbb{R}^n$, $u(t) \in \mathbb{R}$, and $y(t) \in \mathbb{R}$ are the state, control input, and regulated output of the system, respectively. $y_m(t) \in \mathbb{R}$ represents the measured output. $w_I(t)$ and $w_M(t)$ denote the bounded, unstructured input and measurement noise, respectively, satisfying $\|w_I(\cdot)\|_\infty \le \bar{w}_I < \infty$ and $\|w_M(\cdot)\|_\infty \le \bar{w}_M < \infty$. The vector $\mu \in \mathbb{R}^\ell$ collects the uncertain parameters of the plant model, assumed to range over a known compact set $\mathcal{W} \subset \mathbb{R}^\ell$. $A(\mu)$, $B(\mu)$, and $C(\mu)$ are unknown matrices of compatible dimensions. For future use, let $W_\mu(s) := C(\mu)\big(sI - A(\mu)\big)^{-1}B(\mu)$ denote the transfer function. $d(t) \in \mathbb{R}$ is the external sinusoidal disturbance, which is generated by the following exosystem:

$$\begin{aligned} \dot{v}(t) &= Sv(t) \\ d(t) &= \Gamma v(t) \end{aligned} \tag{2}$$

where $v(t) \in \mathbb{R}^2$ is the exosystem state and

$$S := \omega_\star H\,, \quad H := \begin{bmatrix} 0 & 1 \\ -1 & 0 \end{bmatrix}, \quad \Gamma := \begin{bmatrix} 1 & 0 \end{bmatrix}, \tag{3}$$

$\omega_\star \in \mathbb{R}_{>0}$ is the frequency of the sinusoidal disturbance.

In accordance with the IMP, in order to fully cancel the disturbance $d(t)$, it is imperative that we integrate the model of the disturbance into the controller. To this end, both the information of the frequency $\omega_\star$ and the frequency response of the plant over $\omega_\star$ defined as

$$\theta^\top(\omega_\star, \mu) := \big[\mathrm{Re}\big(W_\mu(j\omega_\star)\big)\ \ \mathrm{Im}\big(W_\mu(j\omega_\star)\big)\big]$$

are essential. However, in practical applications, acquiring accurate values of both $\omega_\star$ and $\theta(\omega_\star, \mu)$ is proven to be a formidable task, particularly in the face of system uncertainties and sensor noise. Therefore, in this work, we introduce $\hat{\omega} \in \mathbb{R}_{>0}$ as prior knowledge of $\omega_\star$, which can be obtained through any existing frequency estimator [19]–[21]. However, given the presence of sensor errors, it is inevitable that there will be inaccuracies in $\hat{\omega}$. Consequently, we define the potential *frequency parameter error* as $\tilde{\omega} := \hat{\omega} - \omega_\star \in \mathbb{R}$. Therefore, the unknown parameter vector

$$\hat{\theta}^\top(\hat{\omega}, \mu) = \big[\hat{\theta}_1\ \hat{\theta}_2\big] := \big[\mathrm{Re}\big(W_\mu(j\hat{\omega})\big)\ \ \mathrm{Im}\big(W_\mu(j\hat{\omega})\big)\big]$$

represents the frequency response vector of system (1) at $\hat{\omega}$. Since $\hat{\theta}(\hat{\omega}, \mu)$ is a constant term, without loss of generality, we make the following assumption.

Assumption 1: The unknown parameter vector $\hat{\theta}(\hat{\omega}, \mu)$ satisfies $\hat{\theta}(\hat{\omega}, \mu) \in \Theta$ for all $\mu \in \mathcal{W}$ and $\hat{\omega} \in \mathbb{R}_{>0}$, where $\Theta \subset \mathbb{R}^2$ is a compact annular region given by

$$\Theta := \{\theta \in \mathbb{R}^2 \mid r_1^2 \le \|\theta\|^2 \le r_2^2\} \tag{4}$$

for some known positive numbers $r_2 > r_1 > 0$. ◁

Next, we clarify the statement that system (1) is internally and robustly stable for $\mu \in \mathcal{W}$.

Assumption 2: There exist constants $\lambda_2 > \lambda_1 > 0$ such that the solution $P_A : \mathcal{W} \to \mathbb{R}^{n\times n}$ of the parameterized family of Lyapunov equations

$$A^\top(\mu)P_A(\mu) + P_A(\mu)A(\mu) = -I$$

satisfies $\lambda_1 I \preceq P_A(\mu) \preceq \lambda_2 I$ for all $\mu \in \mathcal{W}$. ◁

Remark 1: In this study, we primarily focus on attenuating the impact of the periodic disturbance, whereby we assume that the amplitude of $d(t)$ significantly surpasses the magnitude of $w_I(t)$ and $w_M(t)$. As for Assumptions 1 and 2, it is always possible to identify sufficiently small r_1 and λ_1, as well as sufficiently large r_2 and λ_2, such that the aforementioned assumptions are satisfied. Moreover, Assumption 2 is a standard assumption for the linear output regulation problem and can be found in [17], [23]. ◁

A. Controller Design

Inspired by previous work [17], we propose the following IM-based AFC for system (1)-(3) to eliminate the influence of the external disturbance $d(t)$:

$$\begin{aligned} \dot{\hat{v}}(t) &= \hat{S}\hat{v}(t) - \varepsilon G\hat{\chi}^\top(t)\hat{\zeta}(t)\,,\ \hat{v}(0) = \hat{v}_0 \in \mathbb{R}^2 \\ u(t) &= \Gamma\hat{v}(t) \end{aligned} \tag{5}$$

where $\hat{v}(t) \in \mathbb{R}^2$ is an estimate of $v(t)$, $\hat{S} := \hat{\omega}H \in \mathbb{R}^{2\times 2}$, $G := \Gamma^\top \in \mathbb{R}^2$, and $\varepsilon > 0$ is a control gain. As there is an estimation process, there is bound to be estimation error. However, since $v(t)$ itself is not directly measurable, obtaining the estimation error is typically not possible. To overcome this challenge, an observer $\hat{\zeta}(t) \in \mathbb{R}^2$ is introduced to correct the estimation error and drive it towards zero:

$$\dot{\hat{\zeta}}(t) = E(t)\hat{\zeta}(t) - \varepsilon G\big[\Gamma\hat{\zeta}(t) - y_m(t)\big]\,,\ \hat{\zeta}(0) = \hat{\zeta}_0 \in \mathbb{R}^2 \tag{6}$$

where $E(t) := \hat{S} - \varepsilon\hat{\chi}(t)\hat{\chi}^\top(t) \in \mathbb{R}^{2\times 2}$, $\hat{\chi}(t) \in \mathbb{R}^2$ is a vector of parameter estimates, whose dynamics admit the following adaptive law:

$$\dot{\hat{\chi}}(t) = \mathcal{S}\Big(\tfrac{-\varepsilon^2\rho}{m^2(t)}\hat{\xi}_1(t)\big[\Gamma\hat{\zeta}(t) - y_m(t)\big]\Big)\,,\ \hat{\chi}(0) = \hat{\chi}_0 \in \mathbb{R}^2 \tag{7}$$

$$\dot{\hat{\xi}}_1(t) = F^\top\hat{\xi}_1(t) - \varepsilon G\hat{\chi}^\top(t)\hat{\zeta}(t)\,,\ \hat{\xi}_1(0) = \hat{\xi}_{10} \in \mathbb{R}^2 \tag{8}$$

where $m^2(t) := 1 + \|\hat{\xi}_1(t)\|^2 + |\Gamma\hat{\zeta}(t) - y_m(t)|^2 \in \mathbb{R}_{>0}$, $F := \hat{S} - \varepsilon G\Gamma \in \mathbb{R}^{2\times 2}$, $\rho > 0$ is an adaptive gain, and $\hat{\xi}_1(t)$ can be viewed as a regressor signal. $\mathcal{S}(\cdot)$ denotes a *multiple-model supervised switching mechanism*, which is proposed in [17]. Due to the space limitation, we omit the detailed description of the switching mechanism and kindly

Manuscript 232 submitted to 2024 American Control Conference (ACC).
Received September 26, 2023.

invite readers to refer to the exact same design and analysis procedure in [17, Section V], from which one can easily verify the following properties of $\hat{\chi}(\cdot)$ and $m(\cdot)$ ensured by the switching mechanism.

Property 1 ([17, Property 3.1]): The signal $\hat{\chi}(\cdot)$ defined on $[0,\infty)$ satisfies $\hat{\chi}(t) \in \Theta$ and $\|\dot{\hat{\chi}}(t)\| \leq \varepsilon^2\rho$ for all $t \geq 0$ and $\hat{\chi}_0 \in \operatorname{int}\Theta$. ◁

Property 2 ([17, Lemma 5.3]): The normalization signal $m(\cdot)$ in the adaptive law (7) belongs to $\mathcal{L}_\infty$. ◁

Similar to the stability analysis presented in [17], it is tedious but not difficult to show that if $\hat{\omega}$ is accurate and the system is free from input and measurement noise, the controller proposed here can completely cancel the external disturbance $d(t)$. However, when confronted with a non-ideal environment, the $\mathcal{L}_2$-to-$\mathcal{L}_\infty$ stability established in [17] fails immediately. Therefore, in this study, we tend to achieve a more practical regulation result, specifically, an efficient attenuation of the major influence brought by $d(t)$, in a more realistic scenario (both the input and output signals are polluted by unstructured noise). Hence, the problem can now be formally formulated as follows:

Problem 1: Suppose Assumptions 1-2 hold. For system (1)-(3) driven by the AFC (5)-(8), prove that all trajectories of the closed-loop system originating from any initial conditions $x(0) \in \mathbb{R}^n$, $v(0) \in \mathbb{R}^2$, $\hat{v}_0, \hat{\zeta}_0, \hat{\chi}_0, \hat{\xi}_{10} \in \mathbb{R}^2$ are bounded; and there exist functions $\beta \in \mathcal{KL}$ and $\alpha_1, \alpha_2, \alpha_3 \in \mathcal{K}_\infty$ such that the regulated output satisfies

$$|y(t)| \leq \beta(\|x(0)\|, t) + \alpha_1(\|\tilde{\omega}\|_{[0,t]}) + \alpha_2(\|w_I\|_{[0,t]}) + \alpha_3(\|w_M\|_{[0,t]})$$

for all $t \geq 0$, where $\|\cdot\|_T$ denotes the supremum norm of a signal over an interval T. ◁

III. Stability and Robustness Analysis

In this section, along with the AFC (5)-(8), we aim to demonstrate the robustness of the closed-loop system and build a clear correlation between the ultimate bound of the regulated output, tuning gains, and the magnitude of perturbations. Specifically, our goal is to establish the ISS property with respect to frequency parameter error $\tilde{\omega}$, input noise $w_I(t)$, and measurement noise $w_M(t)$.

For simplicity and clarity, we will omit the dependence on t in the following formulas. To begin with, we apply a coordinate change as $\tilde{v} := \hat{v} - v \in \mathbb{R}^2$ and $z := x - \Pi(\mu)\tilde{v} \in \mathbb{R}^n$. Letting $\tilde{S} := \tilde{\omega}H \in \mathbb{R}^{2\times 2}$, one obtains the *error system*:

$$\begin{aligned} \dot{z} &= A(\mu)z + \varepsilon\Pi(\mu)G\hat{\chi}^\top\tilde{\zeta} - \Pi(\mu)\tilde{S}v + B(\mu)w_I \\ \dot{\tilde{v}} &= \hat{S}\tilde{v} - \varepsilon G\hat{\chi}^\top\hat{\zeta} + \tilde{S}v \\ y &= C(\mu)z + \hat{\theta}^\top(\hat{\omega},\mu)\tilde{v} \\ y_m &= C(\mu)z + \hat{\theta}^\top(\hat{\omega},\mu)\tilde{v} + w_M \end{aligned} \tag{9}$$

where $\Pi(\mu)$ is the unique solution of the Sylvester equation:

$$\Pi(\mu)\hat{S} = A(\mu)\Pi(\mu) + B(\mu)\Gamma\,.$$

Again, we use the coordinate transformation $\zeta := D^{-1}\tilde{v} \in \mathbb{R}^2$, where $D := \frac{1}{\hat{\theta}_1^2+\hat{\theta}_2^2}\begin{bmatrix}\hat{\theta}_1 & -\hat{\theta}_2 \\ \hat{\theta}_2 & \hat{\theta}_1\end{bmatrix}$, to obtain a more suitable realization:

$$\dot{\zeta} = \hat{S}\zeta - \varepsilon\chi\hat{\chi}^\top\hat{\zeta} + D^{-1}\tilde{S}v\,,$$

where $\chi := \begin{bmatrix}\hat{\theta}_1 & -\hat{\theta}_2\end{bmatrix}^\top \in \mathbb{R}^2$ is also a vector containing the unknown frequency response and satisfies Assumption 1.

For the convenience of analysis, an *auxiliary output* signal

$$y_1 := \Gamma\zeta = \Gamma D^{-1}\tilde{v} = y_m - C(\mu)z - w_M$$

is introduced. Note that, since signals z and w_M are not measurable, y_1 is purely for analysis and not for feedback.

Next, define the observation error $\tilde{\zeta} := \hat{\zeta} - \zeta \in \mathbb{R}^2$ and the parameter estimation error $\tilde{\chi} := \hat{\chi} - \chi \in \mathbb{R}^2$. In virtue of observer (6), the dynamics of $\tilde{\zeta}$ can be expressed as follows:

$$\begin{aligned} \dot{\tilde{\zeta}} &= F\tilde{\zeta} - \varepsilon\tilde{\chi}\hat{\chi}^\top\hat{\zeta} + \varepsilon GC(\mu)z - D^{-1}\tilde{S}v + \varepsilon Gw_M \\ \tilde{y} &= \Gamma\tilde{\zeta} - C(\mu)z - w_M \end{aligned} \tag{10}$$

It should be noted that F is Hurwitz for all $\varepsilon > 0$ (see Lemma 2). In order to demonstrate the stability of the original closed-loop system, it is imperative to ensure that both $\hat{\zeta}$ and ζ are bounded. This is equivalent to proving the stability of $\hat{\zeta}$ and $\tilde{\zeta}$. To this end, it is necessary to develop a non-minimal realization of (10), illustrate the boundedness of all signals in (10), and subsequently verify the robustness of the closed-loop system.

A. Non-minimal Realization

To analyze the impact of frequency parameter error, input noise, and measurement noise separately, system (10) is recast as four parallel connected systems, with input-output maps given, respectively, by

$$\tilde{y}_1(t) = -\varepsilon\Gamma\int_0^t e^{F(t-\tau)}\tilde{\chi}(\tau)\hat{\chi}^\top(\tau)\hat{\zeta}(\tau)\,d\tau \tag{11}$$

$$\tilde{y}_2(t) = \varepsilon\Gamma\int_0^t e^{F(t-\tau)}GC(\mu)z(\tau)\,d\tau - C(\mu)z(t) \tag{12}$$

$$\tilde{y}_3(t) = -\Gamma\int_0^t e^{F(t-\tau)}D^{-1}\tilde{S}v(\tau)\,d\tau \tag{13}$$

$$\tilde{y}_4(t) = \varepsilon\Gamma\int_0^t e^{F(t-\tau)}Gw_M(\tau)d\tau - w_M(t) \tag{14}$$

with $\tilde{y} = \tilde{y}_1 + \tilde{y}_2 + \tilde{y}_3 + \tilde{y}_4$.

Using a suitable version of the classic *Swapping Lemma* in [24], the impulse response of (11) admits a linear time-varying (LTV) realization:

$$\begin{aligned} \dot{\xi}_1 &= F^\top\xi_1 - \varepsilon G\hat{\chi}^\top\hat{\zeta} \\ \dot{\xi}_2 &= F\xi_2 + Q\dot{\hat{\chi}} \\ \dot{Q} &= FQ - \varepsilon\hat{\chi}^\top\hat{\zeta}\cdot I \\ \tilde{y}_1 &= \tilde{\chi}^\top\xi_1 - \Gamma\xi_2 \end{aligned} \tag{15}$$

where $\xi_1 \in \mathbb{R}^2$, $\xi_2 \in \mathbb{R}^2$, and $Q \in \mathbb{R}^{2\times 2}$.

Based on the three inputs of z dynamics (9), we divide z into three subsystems: z_1, z_2, and z_3, with corresponding

outputs $C(\mu)z_1$, $C(\mu)z_2$, and $C(\mu)z_3$. The impulse response of (12) can be represented as a LTI realization of the form:

$$\begin{aligned}
\dot{\xi}_3 &= F\xi_3 + \varepsilon GC(\mu)z_1\,, \quad \dot{z}_1 = A(\mu)z_1 + \varepsilon\Pi(\mu)G\hat{\chi}^\top\hat{\zeta}\\
\dot{\xi}_4 &= F\xi_4 + \varepsilon GC(\mu)z_2\,, \quad \dot{z}_2 = A(\mu)z_2 - \Pi(\mu)\tilde{S}v\\
\dot{\xi}_5 &= F\xi_5 + \varepsilon GC(\mu)z_3\,, \quad \dot{z}_3 = A(\mu)z_3 + B(\mu)w_I\\
\tilde{y}_2 &= \Gamma\xi_3 - C(\mu)z_1 + \Gamma\xi_4 - C(\mu)z_2 + \Gamma\xi_5 - C(\mu)z_3
\end{aligned} \tag{16}$$

where $\xi_3 \in \mathbb{R}^2$, $z_1 \in \mathbb{R}^n$, $\xi_4 \in \mathbb{R}^2$, $z_2 \in \mathbb{R}^n$, $\xi_5 \in \mathbb{R}^2$, and $z_3 \in \mathbb{R}^n$.

Similarly, (13) and (14) also admit the LTI realization:

$$\begin{aligned}
\dot{\xi}_6 &= F\xi_6 - D^{-1}\tilde{S}v \qquad & \dot{\xi}_7 &= F\xi_7 + \varepsilon G w_M\\
\tilde{y}_3 &= \Gamma\xi_6 & \tilde{y}_4 &= \Gamma\xi_7 - w_M
\end{aligned} \tag{17}$$

where $\xi_6 \in \mathbb{R}^2$ and $\xi_7 \in \mathbb{R}^2$.

While the aggregate state $[\xi_2^\top, \xi_3^\top, \xi_4^\top, \xi_5^\top, \xi_6^\top, \xi_7^\top]^\top$ is not available for observation, an open-loop observer for the state ξ_1 can be designed in the form of (8). Referring to (15), it is clear that $\hat{\xi}_1$ will exponentially converge to ξ_1. Substituting ξ_1 with $\hat{\xi}_1$, we have

$$\begin{aligned}
\dot{\hat{\zeta}} &= E\hat{\zeta} - \varepsilon G\tilde{\chi}^\top\hat{\xi}_1 + \varepsilon G\big[\Gamma\xi_2 - \Gamma\xi_3 + C(\mu)z_1\\
&\quad - \Gamma\xi_4 + C(\mu)z_2 - \Gamma\xi_5 + C(\mu)z_3\\
&\quad - \Gamma\xi_6 - \Gamma\xi_7 + w_M + \tilde{\chi}^\top\tilde{\xi}_1\big]\\
\dot{\hat{\xi}}_1 &= F^\top\hat{\xi}_1 - \varepsilon G\hat{\chi}^\top\hat{\zeta}\\
y &= \Gamma\hat{\zeta} - \big[\tilde{\chi}^\top\hat{\xi}_1 - \Gamma\xi_2 + \Gamma\xi_3 - C(\mu)z_1\\
&\quad + \Gamma\xi_4 - C(\mu)z_2 + \Gamma\xi_5 - C(\mu)z_3\\
&\quad + \Gamma\xi_6 + \Gamma\xi_7 - w_M - \tilde{\chi}^\top\tilde{\xi}_1\big] - w_M
\end{aligned} \tag{18}$$

where $\tilde{\xi}_1 := \hat{\xi}_1 - \xi_1 \in \mathbb{R}^2$. Thanks to Lemma 2 and the fact that the boundedness of $\hat{\chi}(\cdot)$ will be enforced by (7), with a minor abuse but no loss of generality, the exponentially decaying term $\tilde{\chi}^\top\tilde{\xi}_1$ will be dropped from (18). Combining (6), (8), (15), (16), and (17), we can obtain the non-minimal realization of the entire *nonlinear closed-loop system*.

B. Stability and Robustness Analysis

To improve the clarity of the presentation, based on the acquired non-minimal realization in Section III-A, we reorganize the closed-loop system as the interconnection of the following linear subsystems (as shown in Fig. 1):

$$\Sigma_1 : \begin{cases} \dot{\hat{\zeta}} = E\hat{\zeta} + \varepsilon G\kappa_1\\ \eta_1 = \hat{\chi}^\top\hat{\zeta} \end{cases} \tag{19}$$

$$\Sigma_2 : \begin{cases} \dot{\xi}_2 = F\xi_2 + Q\dot{\hat{\chi}}\\ \dot{Q} = FQ - \varepsilon\kappa_2\cdot I\\ \eta_2 = \Gamma\xi_2 \end{cases} \tag{20}$$

$$\Sigma_3 : \begin{cases} \dot{\xi}_3 = F\xi_3 + \varepsilon GC(\mu)z_1\\ \dot{z}_1 = A(\mu)z_1 + \varepsilon\Pi(\mu)G\kappa_3\\ \eta_3 = \Gamma\xi_3 - C(\mu)z_1 \end{cases} \tag{21}$$

$$\Sigma_4 : \begin{cases} \dot{\hat{\xi}}_1 = F^\top\hat{\xi}_1 - \varepsilon G\kappa_4\\ \eta_4 = \tilde{\chi}^\top\hat{\xi}_1 \end{cases} \tag{22}$$

$$\Sigma_5 : \begin{cases} \dot{\xi}_4 = F\xi_4 + \varepsilon GC(\mu)z_2\\ \dot{z}_2 = A(\mu)z_2 - \Pi(\mu)\kappa_5\\ \dot{\xi}_6 = F\xi_6 - D^{-1}\kappa_5\\ \eta_5 = \Gamma\xi_4 - C(\mu)z_2 + \Gamma\xi_6 \end{cases} \tag{23}$$

$$\Sigma_6 : \begin{cases} \dot{\xi}_5 = F\xi_5 + \varepsilon GC(\mu)z_3\\ \dot{z}_3 = A(\mu)z_3 + B(\mu)\kappa_6\\ \eta_6 = \Gamma\xi_5 - C(\mu)z_3 \end{cases} \tag{24}$$

$$\Sigma_7 : \begin{cases} \dot{\xi}_7 = F\xi_7 + \varepsilon G\kappa_7\\ \eta_7 = \Gamma\xi_7 - \kappa_7 \end{cases} \tag{25}$$

with $\kappa_1 = \eta_2 - \sum_{i=3}^{7}\eta_i \in \mathbb{R}$, $\kappa_2 = \kappa_3 = \kappa_4 = \eta_1 \in \mathbb{R}$, frequency parameter error $\kappa_5 = \tilde{S}v \in \mathbb{R}^2$, input noise $\kappa_6 = w_I \in \mathbb{R}$, and measurement noise $\kappa_7 = w_M \in \mathbb{R}$. From Fig. 1, it can be seen that proving the stability of the closed-loop system and its robustness to frequency parameter error, input noise, and measurement noise is equivalent to illustrating that subsystems Σ_5-Σ_7 are ISS with respect to κ_5-κ_7 and subsystems Σ_1-Σ_4 are ISS with respect to η_5-η_7. In other words, if we can show that subsystems Σ_1-Σ_7 are ISS with respect to κ_5-κ_7, Problem 1 is solved.

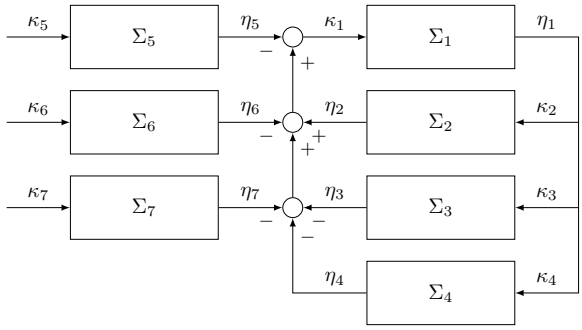

Fig. 1: Interconnection of subsystems Σ_1-Σ_7.

The ISS analysis will be accomplished via Lyapunov functions. Before constructing the Lyapunov function candidate for each subsystem, we first establish the following Lemmas and Property which are instrumental in the ensuing analysis.

Lemma 1: Let $P_E(\chi, \varepsilon)$ denote the solution of the parameterized family of Lyapunov equations

$$E^\top P_E(\chi,\varepsilon) + P_E(\chi,\varepsilon)E = -\varepsilon\chi^\top\chi I\,.$$

There exist scalars $\lambda_4 > \lambda_3 > 0$ such that $P_E : \Theta \times \mathbb{R}_{>0} \to \mathbb{R}^{2\times 2}$ satisfies $\lambda_3 I \preceq P_E(\chi,\varepsilon) \preceq \lambda_4 I$ for all $(\chi,\varepsilon) \in \Theta \times \mathbb{R}_{>0}$. ◁

Lemma 2: Let $P_F(\varepsilon)$ denote the symmetric solution of the family of Lyapunov equations

$$F^\top P_F(\varepsilon) + P_F(\varepsilon)F = -\varepsilon I\,.$$

There exist scalars $\lambda_6 > \lambda_5 > 0$ such that $P_F : \mathbb{R}_{>0} \to \mathbb{R}^{2\times 2}$ satisfies $\lambda_5 I \preceq P_F(\varepsilon) \preceq \lambda_6 I$ for all $\varepsilon \in \mathbb{R}_{>0}$. ◁

The proofs of Lemmas 1 and 2 are given in [17]. Due to space limitations, we omit the detailed procedures here.

Property 3: The gradient with respect to χ of the quadratic form $J_E(q) := q^\top P_E(\chi,\varepsilon)q$, $q \in \mathbb{R}^2$, satisfies $\nabla_\chi J_E(q) = \varepsilon\big[q^\top R_1(\chi,\varepsilon)q \; q^\top R_2(\chi,\varepsilon)q\big]$ for some matrix-valued functions $R_1, R_2 : \Theta \times \mathbb{R}_{>0} \to \mathbb{R}^{2\times 2}$, which are continuous and bounded for all $(\chi,\varepsilon) \in \Theta \times (0,\bar{\varepsilon}_0]$, where $\bar{\varepsilon}_0 > 0$ can be viewed as a boundary for ε. ◁

Proof. Since the entries of P_E are continuously differentiable functions of $\chi = [\chi_1 \; \chi_2]^\top$ over an open neighborhood of Θ, for $q \in \mathbb{R}^2$, the gradient with respect to χ of the quadratic form $J_E(q) := q^\top P_E(\chi,\varepsilon)q$ satisfies

$$\frac{\partial J_E(q)}{\partial \chi} = \varepsilon\big[q^\top R_1(\chi,\varepsilon)q \; q^\top R_2(\chi,\varepsilon)q\big]\,,$$

where $R_i(\chi,\varepsilon) = \varepsilon^{-1}\frac{\partial P_E}{\partial \chi_i}$, $i = 1,2$ are continuous and bounded matrix-valued functions over $\Theta \times (0,\bar{\varepsilon}_0]$. □

Now, the main result of this paper is stated below:

Theorem 1: Suppose that Assumptions 1-2 hold. For system (1)-(3) governed by the proposed AFC (5)-(8), there exist scalars $\bar{\varepsilon} > 0$ and $\underline{\rho} > 0$ such that for all $\varepsilon \in (0,\bar{\varepsilon})$ and $\rho \geq \underline{\rho}$, Problem 1 is solved. ◁

Proof. To analyze the ISS property of the closed-loop system, we establish the corresponding Lyapunov function candidate for each subsystem Σ_1-Σ_7.

1) Evaluating the derivative of the Lyapunov function candidate $V_1(t,\hat{\zeta}) := \hat{\zeta}^\top P_E(\hat{\chi}(t),\varepsilon)\hat{\zeta}$ along the trajectories of subsystem Σ_1 yields, for all $(\hat{\chi},\varepsilon) \in \Theta \times \mathbb{R}_{>0}$

$$\begin{aligned}\dot{V}_1 &= -\varepsilon\hat{\zeta}^\top\hat{\chi}^\top\hat{\chi}\hat{\zeta} + \frac{\partial \hat{\zeta}^\top P_E(\hat{\chi},\varepsilon)\hat{\zeta}}{\partial \hat{\chi}}\dot{\hat{\chi}} + 2\varepsilon\hat{\zeta}^\top P_E(\hat{\chi},\varepsilon)G\kappa_1 \\ &\leq -\varepsilon r_1^2\|\hat{\zeta}\|^2 + \varepsilon^3\rho\sigma_1\|\hat{\zeta}\|^2 + 2\varepsilon\lambda_4\|\hat{\zeta}\||\kappa_1|\,,\end{aligned} \tag{26}$$

where we used Lemma 1, Properties 1 and 3. r_1 is defined in (4), and σ_1 is denoted by the quantity

$$\sigma_1 := \max_{\hat{\chi}(\cdot)\in\Theta,\varepsilon\in(0,\bar{\varepsilon}_0]}\big\{\|R_1(\hat{\chi},\varepsilon)\| + \|R_2(\hat{\chi},\varepsilon)\|\big\}\,.$$

After substituting $\kappa_1 = \eta_2 - \sum_{i=3}^7 \eta_i$ into (26), and making use of Young's inequality for the cross terms, one obtains

$$\begin{aligned}\dot{V}_1 \leq -\varepsilon\Big(\frac{r_1^2}{12} - \varepsilon^2\rho\sigma_1\Big)\|\hat{\zeta}\|^2 + 12\varepsilon\lambda_4^2 r_1^{-2}\big(\|\xi_2\|^2 + \|\xi_3\|^2 \\ + \sigma_2\|z_1\|^2 + |\tilde{\chi}^\top\hat{\xi}_1|^2 + \|\xi_4\|^2 + \sigma_2\|z_2\|^2 + \|\xi_6\|^2 \\ + \|\xi_5\|^2 + \sigma_2\|z_3\|^2 + \|\xi_7\|^2 + |\kappa_7|^2\big)\,,\end{aligned}$$

where $\sigma_2 := \max_{\mu\in\mathcal{W}}\|C(\mu)\|^2$.

2) Next, consider the Lyapunov function candidate $V_2(\xi_2,Q) := \varepsilon^{-1}\xi_2^\top P_F(\varepsilon)\xi_2 + a(\varepsilon)\varepsilon^{-1}\operatorname{trace}\big(Q^\top P_F(\varepsilon)Q\big)$ for subsystem Σ_2, where $a(\varepsilon)$ is a positive number to be determined. The time derivative of V_2 along the trajectories of Σ_2 yields, for all $(\hat{\chi},\varepsilon) \in \Theta \times \mathbb{R}_{>0}$

$$\begin{aligned}\dot{V}_2 &= -\|\xi_2\|^2 + 2\varepsilon^{-1}\xi_2^\top P_F(\varepsilon)Q\dot{\hat{\chi}} \\ &\quad + a(\varepsilon)\big[-\|Q\|_F^2 - 2\operatorname{trace}\big(Q^\top P_F(\varepsilon)\big)\kappa_2\big] \\ &\leq -\frac{1}{2}\|\xi_2\|^2 - \frac{a(\varepsilon)}{4}\|Q\|_F^2 \\ &\quad - \Big(\frac{a(\varepsilon)}{4} - 2\varepsilon^2\rho^2\lambda_6^2\Big)\|Q\|_F^2 + 4a(\varepsilon)\lambda_6^2|\kappa_2|^2\,.\end{aligned}$$

Setting $a(\varepsilon) := 8\varepsilon^2\rho^2\lambda_6^2$ and substituting the input κ_2 with $\hat{\chi}^\top\hat{\zeta}$ yields:

$$\dot{V}_2 \leq -\frac{1}{2}\|\xi_2\|^2 - 2\varepsilon^2\rho^2\lambda_6^2\|Q\|_F^2 + 32\varepsilon^2\rho^2\lambda_6^4 r_2^2\|\hat{\zeta}\|^2\,.$$

3) Similarly, for Σ_3, evaluating the time derivative of the Lyapunov function candidate $V_3(\xi_3,z_1) := \varepsilon^{-1}\xi_3^\top P_F(\varepsilon)\xi_3 + b_1 z_1^\top P_A(\mu)z_1$, where $b_1 > 0$ is a constant to be determined, one has

$$\begin{aligned}\dot{V}_3 &= -\|\xi_3\|^2 + 2\xi_3^\top P_F(\varepsilon)GC(\mu)z_1 \\ &\quad + b_1\big(-\|z_1\|^2 + 2\varepsilon z_1^\top P_A(\mu)\Pi(\mu)G\kappa_3\big) \\ &\leq -\frac{1}{2}\|\xi_3\|^2 - \frac{b_1}{4}\|z_1\|^2 \\ &\quad - \Big(\frac{b_1}{4} - 2\lambda_6^2\sigma_2\Big)\|z_1\|^2 + b_1\varepsilon^2\sigma_3|\kappa_3|^2\,,\end{aligned}$$

where $\sigma_3 := \max_{\mu\in\mathcal{W}} 2\lambda_2^2\|\Pi(\mu)\|^2$. By setting $b_1 := 8\lambda_6^2\sigma_2$ and substituting $\kappa_3 = \hat{\chi}^\top\hat{\zeta}$, we obtain

$$\dot{V}_3 \leq -\frac{1}{2}\|\xi_3\|^2 - 2\lambda_6^2\sigma_2\|z_1\|^2 + 8\varepsilon^2\lambda_6^2\sigma_2\sigma_3 r_2^2\|\hat{\zeta}\|^2\,.$$

4) Consider the Lyapunov function candidate $V_4(\hat{\xi}_1) := \varepsilon\hat{\xi}_1^\top P_{F^\top}(\varepsilon)\hat{\xi}_1$, where $P_{F^\top}(\varepsilon)$ satisfies the exact Lyapunov equation result in Lemma 2. Evaluating the time derivative of V_4 along the trajectories of Σ_4 yields

$$\begin{aligned}\dot{V}_4 &= -\varepsilon^2\|\hat{\xi}_1\|^2 - 2\varepsilon^2\hat{\xi}_1^\top P_{F^\top}(\varepsilon)G\kappa_4 \\ &\leq -\varepsilon^2\|\hat{\xi}_1\|^2 + 2\varepsilon^2\lambda_6\|\hat{\xi}_1\||\kappa_4| \\ &\leq -\frac{\varepsilon^2}{2}\|\hat{\xi}_1\|^2 + 2\varepsilon^2\lambda_6^2 r_2^2\|\hat{\zeta}\|^2\,.\end{aligned}$$

5) The Lyapunov function candidate $V_5(\xi_4,z_2,\xi_6) := \varepsilon^{-1}\xi_4^\top P_F(\varepsilon)\xi_4 + b_2 z_2^\top P_A(\mu)z_2 + \varepsilon^{-1}\xi_6^\top P_F(\varepsilon)\xi_6$ is built for Σ_5, where $b_2 > 0$ is a constant to be determined. Computing its derivative along the corresponding trajectories, it yields

$$\begin{aligned}\dot{V}_5 &= -\|\xi_4\|^2 + 2\xi_4^\top P_F(\varepsilon)GC(\mu)z_2 \\ &\quad + b_2\big(-\|z_2\|^2 - 2z_2^\top P_A(\mu)\Pi(\mu)\kappa_5\big) \\ &\quad - \|\xi_6\|^2 - 2\varepsilon^{-1}\xi_6^\top P_F(\varepsilon)D^{-1}\kappa_5 \\ &\leq -\frac{1}{2}\|\xi_4\|^2 - \frac{b_2}{4}\|z_2\|^2 - \frac{1}{2}\|\xi_6\|^2 \\ &\quad - \Big(\frac{b_2}{4} - 2\lambda_6^2\sigma_2\Big)\|z_2\|^2 + (b_2\sigma_3 + 2\varepsilon^{-2}\lambda_6^2 r_2^2)\|\kappa_5\|^2\,,\end{aligned}$$

where we used the fact $\|D^{-1}\|^2 = \|\hat{\chi}\|^2 \leq r_2^2$. Setting $b_2 := 8\lambda_6^2\sigma_2$ as well, the following holds:

$$\begin{aligned}\dot{V}_5 \leq -\frac{1}{2}\|\xi_4\|^2 - 2\lambda_6^2\sigma_2\|z_2\|^2 - \frac{1}{2}\|\xi_6\|^2 \\ + (8\lambda_6^2\sigma_2\sigma_3 + 2\varepsilon^{-2}\lambda_6^2 r_2^2)\|\kappa_5\|^2\,.\end{aligned}$$

6) Now we propose the Lyapunov function candidate for Σ_6 as $V_6(\xi_5,z_3) := \varepsilon^{-1}\xi_5^\top P_F(\varepsilon)\xi_5 + b_3 z_3^\top P_A(\mu)z_3$. Here, b_3 is a positive constant that will be determined. Evaluating its derivative, one gets

$$\begin{aligned}\dot{V}_6 &\leq -\|\xi_5\|^2 + 2\xi_5^\top P_F(\varepsilon)GC(\mu)z_3 \\ &\quad + b_3\big(-\|z_3\|^2 + 2z_3^\top P_A(\mu)B(\mu)\kappa_6\big) \\ &\leq -\frac{1}{2}\|\xi_5\|^2 - \frac{b_3}{4}\|z_3\|^2 \\ &\quad - \Big(\frac{b_3}{4} - 2\lambda_6^2\sigma_2\Big)\|z_3\|^2 + b_3\sigma_4|\kappa_6|^2\,,\end{aligned}$$

Manuscript 232 submitted to 2024 American Control Conference (ACC).
Received September 26, 2023.

where $\sigma_4 := \max_{\mu\in\mathcal{W}} 2\lambda_2^2\|B(\mu)\|^2$. Letting $b_3 := 8\lambda_6^2\sigma_2$, it results in

$$\dot{V}_6 \le -\frac{1}{2}\|\xi_5\|^2 - 2\lambda_6^2\sigma_2\|z_3\|^2 + 8\lambda_6^2\sigma_2\sigma_4|\kappa_6|^2\,.$$

7) Consider $V_7(\xi_7) := \varepsilon^{-1}\xi_7^\top P_F(\varepsilon)\xi_7$ for Σ_7. Computing its derivative along the trajectories of Σ_7, it follows

$$\begin{aligned}\dot{V}_7 &= -\|\xi_7\|^2 + 2\xi_7^\top P_F(\varepsilon)G\kappa_7\\ &\le -\|\xi_7\|^2 + 2\lambda_6\|\xi_7\||\kappa_7|\\ &\le -\frac{1}{2}\|\xi_7\|^2 + 2\lambda_6^2|\kappa_7|^2\,.\end{aligned}$$

8) Furthermore, we establish a Lyapunov function candidate for the estimation error $\tilde{\chi}$. Consider the storage function $V_8(\tilde{\chi}) := \varepsilon^{-1}\tilde{\chi}^\top\tilde{\chi}$. Evaluating the derivative of V_8 along the trajectories of the parameter estimate (7) yields

$$\dot{V}_8 = -2\varepsilon\rho\tilde{\chi}^\top\frac{\hat{\xi}_1\tilde{y}}{m^2}\,. \tag{27}$$

Substituting $\tilde{y} = \hat{\xi}_1^\top\tilde{\chi} - \eta_2 + \sum_{i=3}^{7}\eta_i$ into (27), one derives

$$\begin{aligned}\dot{V}_8 &\le -2\varepsilon\rho\tilde{\chi}^\top\frac{\hat{\xi}_1(\hat{\xi}_1^\top\tilde{\chi} - \eta_2 + \eta_3 + \eta_5 + \eta_6 + \eta_7)}{m^2}\\ &\le -\frac{\varepsilon\rho}{3\|m\|_\infty^2}|\tilde{\chi}^\top\hat{\xi}_1|^2 + 3\varepsilon\rho\big(\|\xi_2\|^2 + 2\|\xi_3\|^2 + 2\sigma_2\|z_1\|^2\\ &\quad + 3\|\xi_4\|^2 + 3\sigma_2\|z_2\|^2 + 3\|\xi_6\|^2 + 2\|\xi_5\|^2 + 2\sigma_2\|z_3\|^2\\ &\quad + 2\|\xi_7\|^2 + 2|\kappa_7|^2\big)\,.\end{aligned}$$

Finally, we are in the position to show that the closed-loop system is ISS with respect to κ_5-κ_7. Let $V = \sum_{i=1}^{8}V_i$ be the overall Lyapunov function candidate. Evaluating its derivative along the trajectories of all subsystems, we can establish the following result:

$$\begin{aligned}\dot{V} \le\ & -\varepsilon\Big(\frac{r_1^2}{12} - \varepsilon^2\rho\sigma_1 - 32\varepsilon\rho^2\lambda_6^4 r_2^2 - 8\varepsilon\lambda_6^2\sigma_2\sigma_3 r_2^2 - 2\varepsilon\lambda_6^2 r_2^2\Big)\|\hat{\zeta}\|^2\\ & - \Big(\frac{1}{2} - 12\varepsilon\lambda_4^2 r_1^{-2} - 3\varepsilon\rho\Big)\|\xi_2\|^2 - 2\varepsilon^2\rho^2\lambda_6^2\|Q\|_F^2\\ & - \Big(\frac{1}{2} - 12\varepsilon\lambda_4^2 r_1^{-2} - 6\varepsilon\rho\Big)\|\xi_3\|^2\\ & - \big(2\lambda_6^2\sigma_2 - 12\varepsilon\lambda_4^2\sigma_2 r_1^{-2} - 6\varepsilon\rho\sigma_2\big)\|z_1\|^2\\ & - \frac{\varepsilon^2}{2}\|\hat{\xi}_1\|^2 - \varepsilon\Big(\frac{\rho}{3\|m\|_\infty^2} - 12\lambda_4^2 r_1^{-2}\Big)|\tilde{\chi}^\top\hat{\xi}_1|^2\\ & - \Big(\frac{1}{2} - 12\varepsilon\lambda_4^2 r_1^{-2} - 9\varepsilon\rho\Big)\|\xi_4\|^2\\ & - \big(2\lambda_6^2\sigma_2 - 12\varepsilon\lambda_4^2\sigma_2 r_1^{-2} - 9\varepsilon\rho\sigma_2\big)\|z_2\|^2\\ & - \Big(\frac{1}{2} - 12\varepsilon\lambda_4^2 r_1^{-2} - 9\varepsilon\rho\Big)\|\xi_6\|^2\\ & - \Big(\frac{1}{2} - 12\varepsilon\lambda_4^2 r_1^{-2} - 6\varepsilon\rho\Big)\|\xi_5\|^2\\ & - \big(2\lambda_6^2\sigma_2 - 12\varepsilon\lambda_4^2\sigma_2 r_1^{-2} - 6\varepsilon\rho\sigma_2\big)\|z_3\|^2\\ & - \Big(\frac{1}{2} - 12\varepsilon\lambda_4^2 r_1^{-2} - 6\varepsilon\rho\Big)\|\xi_7\|^2\\ & + \big(8\lambda_6^2\sigma_2\sigma_3 + 2\varepsilon^{-2}\lambda_6^2 r_2^2\big)\|\kappa_5\|^2 + 8\lambda_6^2\sigma_2\sigma_4|\kappa_6|^2\\ & + \big(12\varepsilon\lambda_4^2 r_1^{-2} + 6\varepsilon\rho\big)|\kappa_7|^2\,.\end{aligned} \tag{28}$$

Let $\underline{\rho} := 36\lambda_4^2 r_1^{-2}\|m\|_\infty^2$ and $\rho \ge \underline{\rho}$. Given that the range of ε is much less than 1, we can replace ε^2 with ε in (28). With a slight abuse of notation, one can rewrite (28) into the following form:

$$\begin{aligned}\dot{V} \le\ & -\varepsilon\Big(\frac{r_1^2}{12} - c_1\varepsilon\Big)\|\hat{\zeta}\|^2 - \Big(\frac{1}{2} - c_2\varepsilon\Big)\|\xi_2\|^2\\ & - 2\varepsilon^2\rho^2\lambda_6^2\|Q\|_F^2 - \Big(\frac{1}{2} - c_3\varepsilon\Big)\|\xi_3\|^2\\ & - \big(2\lambda_6^2\sigma_2 - c_4\sigma_2\varepsilon\big)\|z_1\|^2 - \frac{\varepsilon^2}{2}\|\hat{\xi}_1\|^2 - \frac{\varepsilon(\rho-\underline{\rho})}{3\|m\|_\infty^2}|\tilde{\chi}^\top\hat{\xi}_1|^2\\ & - \Big(\frac{1}{2} - c_5\varepsilon\Big)\|\xi_4\|^2 - \big(2\lambda_6^2\sigma_2 - c_6\sigma_2\varepsilon\big)\|z_2\|^2\\ & - \Big(\frac{1}{2} - c_5\varepsilon\Big)\|\xi_6\|^2 - \Big(\frac{1}{2} - c_3\varepsilon\Big)\|\xi_5\|^2\\ & - \big(2\lambda_6^2\sigma_2 - c_4\sigma_2\varepsilon\big)\|z_3\|^2 - \Big(\frac{1}{2} - c_3\varepsilon\Big)\|\xi_7\|^2\\ & + \big(8\lambda_6^2\sigma_2\sigma_3 + 2\varepsilon^{-2}\lambda_6^2 r_2^2\big)\|\kappa_5\|^2 + 8\lambda_6^2\sigma_2\sigma_4|\kappa_6|^2\\ & + \big(12\varepsilon\lambda_4^2 r_1^{-2} + 6\varepsilon\rho\big)|\kappa_7|^2\,,\end{aligned} \tag{29}$$

where c_i, $i = 1,\ldots,6$, are all positive constants mainly depending on ρ and μ. Let

$$\bar{\varepsilon} := \min\Big\{\bar{\varepsilon}_0, \frac{r_1^2}{12c_1}, \frac{1}{2c_2}, \frac{1}{2c_3}, \frac{2\lambda_6^2}{c_4}, \frac{1}{2c_5}, \frac{2\lambda_6^2}{c_6}\Big\}\,,$$

if a $\rho \ge \underline{\rho}$ is fixed, then for all $\varepsilon \in (0, \bar{\varepsilon})$, one can easily verify that the closed-loop system is ISS with respect to frequency parameter error κ_5, input noise κ_6, and measurement noise κ_7. Reverting back to (18), it is easy to see that all states contained in $y(t)$ are ISS with respect to κ_5, κ_6, and κ_7. Therefore, it is clear that there exist functions $\beta \in \mathcal{KL}$ and $\alpha_1, \alpha_2, \alpha_3 \in \mathcal{K}_\infty$ such that Problem 1 is solved. □

Remark 2: The main result presented here is a practical regulation result [25], while also containing the asymptotic regulation property claimed in the ideal scenario [17]. Moreover, from the ISS expression given in (29), one can easily see that the ultimate bound of $y(t)$ can be adjusted with control parameters ε and ρ. Specifically, decreasing ε will improve the robustness of the algorithm to input and measurement noise. However, correspondingly, higher frequency accuracy will be required to achieve better attenuation. ◁

IV. Simulation and Experimental Results

This section serves to validate the claimed stability and robustness properties of the proposed adaptive controller. Simulations and experiments are conducted to demonstrate its practical applicability in real-world scenarios.

A. Numerical Simulation

The numerical simulation is performed on the plant model characterized by a stable and non-minimum phase transfer function *(which is assumed to be unknown)*:

$$W_\mu(s) = \frac{2(s-1)}{s^2 + 2s + 5}\,.$$

The frequency $\omega_\star$ of the disturbance $d(t)$ is set to $\omega_\star = 3\,\mathrm{rad/s}$. The initial condition $v(0)$ of the exosystem is randomly selected from the interval $(-1, 1)$. The control gains of the AFC are chosen as $\varepsilon = 0.5$, $\rho = 0.5$, $r_1 = 0.2$, $r_2 = 2$. The initial conditions of all states of the controller

are set to zero, except for the parameter estimate $\hat{\chi}_0$, which is initialized as $\hat{\chi}_0 = \left[\sqrt{3}/2\ 1/2\right]^\top$. The parameters of the switching mechanism $\mathcal{S}(\cdot)$ are set to the same values as in [17]. $w_I(t)$ and $w_M(t)$ applied are normally distributed random variables.

The simulation results are reported in Figs. 2-3, which show the time history of the measured output $y_m(t)$ and the regulated output $y(t)$ under different scenarios.

As depicted in Fig. 2, in the case where the system is only subjected to the external disturbance $d(t)$, the output of the system rapidly converges to zero, which is referred to as the "ideal" case. Keeping all the settings untouched, one can still observe that, even under significant perturbations, i.e. under the effects of frequency parameter error, input noise, and measurement noise simultaneously, the measured output can still be kept within a relatively small bound, indicating that our controller exhibits strong robustness.

Furthermore, the sensitivity of the presented AFC with respect to the frequency parameter error is shown in Fig. 3. It indicates that the attenuation ability of the regulator is proportional to the size of the parameter error $\tilde{\omega}$ when the parameter error is relatively small. Interestingly, even for a *completely wrong* frequency guess, similar ultimate bounds of the system output can still be ensured. This suggests a potential notch filter property of the presented algorithm.

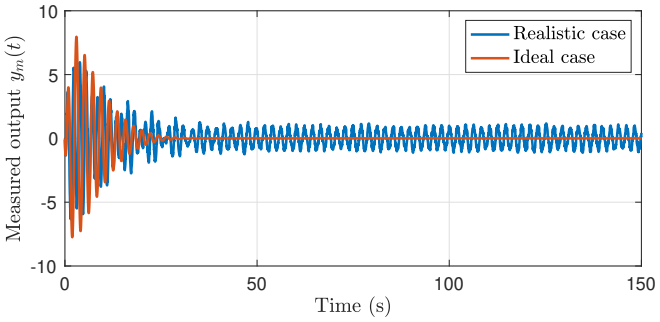

Fig. 2: Realistic case: the system is affected by frequency parameter error $\tilde{\omega} = 1$, unstructured input noise $\bar{w}_I = 0.2$ and unstructured measurement noise $\bar{w}_M = 0.2$. Ideal case: the system is only under the effect of $d(t)$.

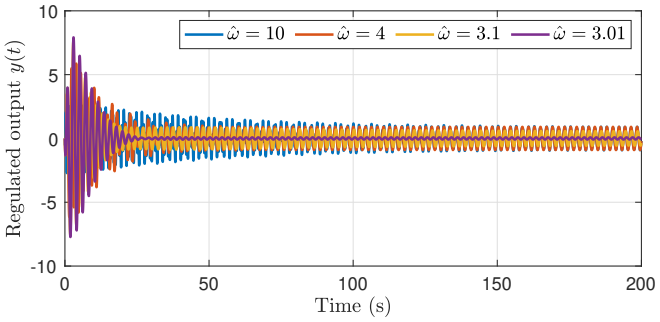

Fig. 3: Regulated output $y(t)$ under different frequency prior knowledge $\hat{\omega}$.

B. Hardware Experiment

To provide a comprehensive evaluation of the proposed approach, we conduct hardware experiments to illustrate its effectiveness in practical scenarios. As depicted in Fig. 4, our experimental setup includes a disturbance speaker, a control speaker, and two microphones. An acoustic duct module is specifically designed with two separate paths to handle the disturbance and control signals. The acoustic module is equipped with multiple microphones, enabling the creation of different *unknown* systems by adjusting the microphone selection. It is worth noting that due to inherent constraints in the speaker's performance and potential inaccuracies in microphone measurements, the system encounters unknown yet bounded frequency parameter error, input noise, and measurement noise. For the experiments, the control gains ε and ρ are set to 0.05 and 0.3 respectively, while keeping the remaining parameters consistent with those used in the simulations. The sampling time is configured to $0.002\,\mathrm{s}$.

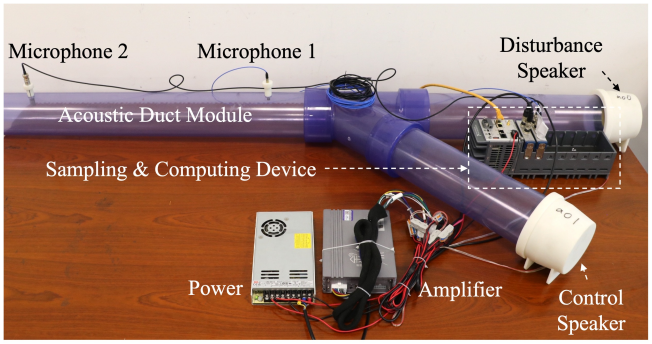

Fig. 4: The prototyped hardware experimental setup.

Fig. 5 presents the convergence behavior in the time domain for disturbances of various frequencies under realistic conditions. Noteworthy disturbance rejection is achieved for each specific frequency within 5 seconds and the final suppression effect can be made consistent by adjusting the parameters. This outcome stands as a testament to the effectiveness of the controller in mitigating external disturbances in real-world scenarios. The demonstration video can be accessed through `https://youtu.be/znoQZ-vOAWA`.

As shown in Fig. 4, disparate microphone positions signify distinct environmental settings. Fig. 6 illustrates that, within the initial 15 seconds, the measured output is acquired via microphone 1, and efficient suppresion of disturbance at $\omega_\star = 634\pi\,\mathrm{rad/s}$ is attained in a short time. At the 15th second, there is a seamless transition to receiving information from microphone 2, and the disturbance is successfully eliminated again. Notably, the achieved rejection performance remains consistent before and after the transition, thereby showcasing the remarkable adaptability and generality of our approach within unknown environments and diverse systems.

Similar to Fig. 3, the robustness performance of the proposed AFC under different frequency prior knowledge conditions is demonstrated in Fig. 7. In this case, the disturbance frequency is set to $\omega_\star = 834\pi\,\mathrm{rad/s}$. Evidently, the ultimate bound of the measured output is directly proportional to the frequency parameter error. However, even when there is a significant difference between acquired prior knowledge $\hat{\omega}$ and the actual frequency $\omega_\star$, the measured output can still be skillfully manipulated within a small range.

Manuscript 232 submitted to 2024 American Control Conference (ACC).
Received September 26, 2023.

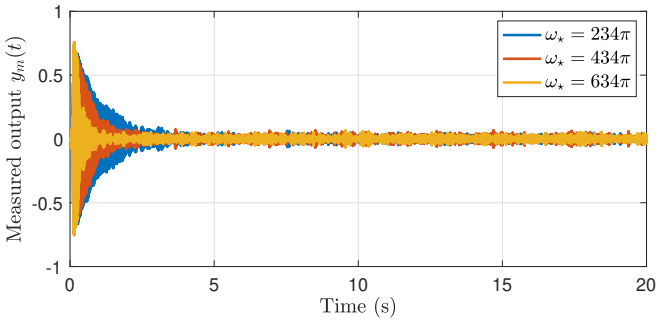

Fig. 5: Time history of the measured output $y_m(t)$ under sinusoidal disturbances at different frequencies $\omega_\star$ in real-world scenarios.

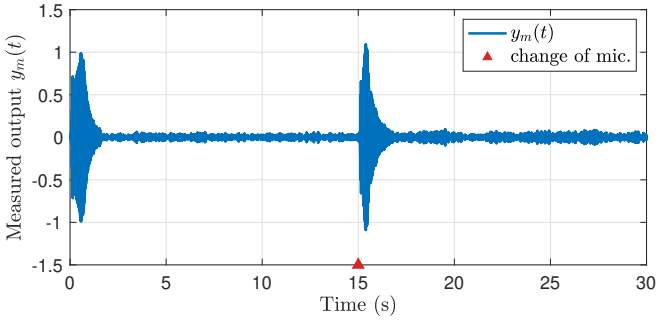

Fig. 6: Disturbance rejection performance for distinct completely unknown systems.

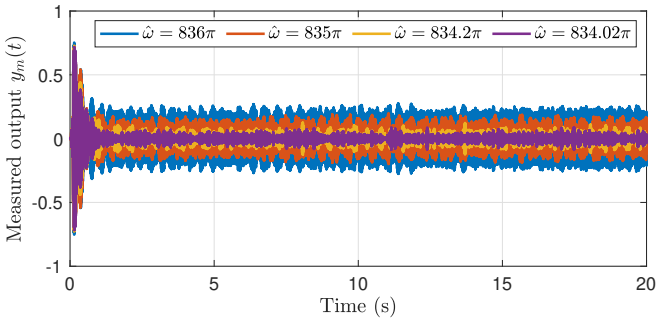

Fig. 7: Measured output $y_m(t)$ under different frequency prior knowledge $\hat{\omega}$.

V. Conclusion

This paper has presented a robust IM-based adaptive feedforward algorithm for rejecting periodic disturbances in uncertain LTI systems. Through rigorous Lyapunov analysis, the ISS property is proven, taking into account the disturbance frequency parameter error, input noise, and measurement noise. The proposed method allows for applications in practical scenarios with significant plant uncertainties, modeling errors, and stochastic effects. Numerical simulations and experimental case studies conducted on an ANC platform have verified the algorithm's performance under unknown and real-world dynamics. Ongoing work involves integrating the proposed technique with frequency estimators. This study holds great potential for real-world engineering applications where robustness is critical, but precise disturbance models are unavailable.

References

[1] G. Garofalo, J. Englsberger, and C. Ott, "On the regulation of the energy of elastic joint robots: Excitation and damping of oscillations," in *Proc. Amer. Control Conf. (ACC)*, 2015, pp. 4825–4831.

[2] A. T. Tran, N. Sakamoto, M. Sato, and K. Muraoka, "Control augmentation system design for quad-tilt-wing unmanned aerial vehicle via robust output regulation method," *IEEE Trans. Aerosp. Electron. Syst.*, vol. 53, no. 1, pp. 357–369, 2017.

[3] B. Francis and W. Wonham, "The internal model principle of control theory," *Automatica*, vol. 12, no. 5, pp. 457–465, 1976.

[4] E. Davison, "The robust control of a servomechanism problem for linear time-invariant multivariable systems," *IEEE Trans. Autom. Control*, vol. 21, no. 1, pp. 25–34, 1976.

[5] M. Lu and J. Huang, "Robust output regulation problem for linear systems with both input and communication delays," in *Proc. Amer. Control Conf. (ACC)*, 2015, pp. 4036–4041.

[6] D. Liang and J. Huang, "Robust output regulation of linear systems by event-triggered dynamic output feedback control," *IEEE Trans. Autom. Control*, vol. 66, no. 5, pp. 2415–2422, 2021.

[7] H. K. Khalil, "Extended high-gain observers as disturbance estimators," *SICE J. Control Meas. Syst. Integr.*, vol. 10, no. 3, pp. 125–134, 2017.

[8] R. Chi, Y. Hui, B. Huang, and Z. Hou, "Active disturbance rejection control for nonaffined globally lipschitz nonlinear discrete-time systems," *IEEE Trans. Autom. Control*, vol. 66, no. 12, pp. 5955–5967, 2021.

[9] K. Ariyur and M. Krstic, "Feedback attenuation and adaptive cancellation of blade vortex interaction on a helicopter blade element," *IEEE Trans. Control Syst. Technol.*, vol. 7, no. 5, pp. 596–605, 1999.

[10] M. Bodson, J. Jensen, and S. Douglas, "Active noise control for periodic disturbances," *IEEE Trans. Control Syst. Technol.*, vol. 9, no. 1, pp. 200–205, 2001.

[11] J. Chandrasekar, L. Liu, D. Patt, P. Friedmann, and D. Bernstein, "Adaptive harmonic steady-state control for disturbance rejection," *IEEE Trans. Control Syst. Technol.*, vol. 14, no. 6, pp. 993–1007, 2006.

[12] S. Pigg and M. Bodson, "Adaptive algorithms for the rejection of sinusoidal disturbances acting on unknown plants," *IEEE Trans. Control Syst. Technol.*, vol. 18, no. 4, pp. 822–836, 2010.

[13] R. Marino and P. Tomei, "Output regulation for unknown stable linear systems," *IEEE Trans. Autom. Control*, vol. 60, no. 8, pp. 2213–2218, 2015.

[14] ——, "Hybrid adaptive multi-sinusoidal disturbance cancellation," *IEEE Trans. Autom. Control*, vol. 62, no. 8, pp. 4023–4030, 2017.

[15] ——, "Adaptive output regulation for minimum-phase systems with unknown relative degree," *Automatica*, vol. 130, p. 109670, 2021.

[16] P. Tomei and R. Marino, "Adaptive regulation for minimum phase systems with unknown relative degree and uncertain exosystems," *Automatica*, vol. 147, p. 110678, 2023.

[17] Y. Wang, G. Pin, A. Serrani, and T. Parisini, "Removing spr-like conditions in adaptive feedforward control of uncertain systems," *IEEE Trans. Autom. Control*, vol. 65, no. 6, pp. 2309–2324, 2020.

[18] P. Bernard, M. Bin, and L. Marconi, "Adaptive output regulation via nonlinear luenberger observer-based internal models and continuous-time identifiers," *Automatica*, vol. 122, p. 109261, 2020.

[19] G. Pin, B. Chen, and T. Parisini, "Robust finite-time estimation of biased sinusoidal signals: A volterra operators approach," *Automatica*, vol. 77, pp. 120–132, 2017.

[20] S. Shi, H. Min, and S. Ding, "Observer-based adaptive scheme for fixed-time frequency estimation of biased sinusoidal signals," *Automatica*, vol. 127, p. 109559, 2021.

[21] D. Wu, S. Li, H. Du, and J. Na, "A finite-time observer-based identification of sinusoidal signal with unknown frequency," *IEEE Trans. Ind. Informat.*, vol. 18, no. 11, pp. 7435–7443, 2022.

[22] Y. Wang, G. Pin, A. Serrani, and T. Parisini, "Removing spr-like conditions in adaptive feedforward control of uncertain systems," in *Proc. 55th IEEE Conf. Decis. Control (CDC)*, 2016, pp. 4728–4733.

[23] W. Liu and J. Huang, "Output regulation of linear systems via sampled-data control," *Automatica*, vol. 113, p. 108684, 2020.

[24] P. Ioannou and J. Sun, *Robust Adaptive Control*. Courier Corporation, 2013.

[25] M. Bin, D. Astolfi, and L. Marconi, "About robustness of control systems embedding an internal model," *IEEE Trans. Autom. Control*, vol. 68, no. 3, pp. 1306–1320, 2023.